Ciemat 713
Sp ISSN 614-087-X

RADIAL PROFILE OF THE ELECTRON DISTRIBUTION FROM ELECTRON CYCLOTRON EMISSION MEASUREMENTS

Tribaldos, V.
Krivenski, V.

CENTRO DE INVESTIGACIONES
ENERGETICAS, MEDIOAMBIENTALES Y TECNOLOGICAS

MADRID, 1993

CLASIFICACION DOE Y DESCRIPTORES

700350
CYCLOTRON RADIATION
ELECTRON CYCLOTRON-RESONANCE
DISTRIBUTION FUNCTIONS
HYBRID SYSTEMS
CURRENT-DRIVE HEATING
NUMERICAL ANALYSIS

Toda correspondencia en relación con este trabajo debe dirigirse al Servicio de Información y Documentación, Centro de Investigaciones Energéticas, Medioambientales y Tecnológicas, Ciudad Universitaria, 28040-MADRID, ESPAÑA.

Las solicitudes de ejemplares deben dirigirse a este mismo Servicio.

Los descriptores se han seleccionado del Thesauro del DOE para describir las materias que contiene este informe con vistas a su recuperación. La catalogación se ha hecho utilizando el documento DOE/TIC-4602 (Rev. 1) Descriptive Cataloguing On-Line, y la clasificación de acuerdo con el documento DOE/TIC.4584-R7 Subject Categories and Scope publicados por el Office of Scientific and Technical Information del Departamento de Energía de los Estados Unidos.

Este trabajo se ha recibido para su impresión en Enero de 1.993.

Depósito Legal nº M-2118-1993
I.S.B.N. 84-7834-183-8
ISSN 614-087-X

IMPRIME CIEMAT

Radial Profile of the Electron Distribution from Electron Cyclotron Emission Measurements

V. Tribaldos and V. Krivenski

Asociación EURATOM-CIEMAT para Fusión, CIEMAT
Avda. Complutense 22, 28040 Madrid, Spain

ABSTRACT

A numerical study is presented, showing the possibility to invert the electron distribution function from a small set of non-thermal emission spectra, for a regime of lower hybrid current drive.

1. INTRODUCTION

When a macroscopic phenomenon is generated by a microscopic process, reconstructing the details of the microscopic process, from the macroscopic effect, is usually a daunting task. However, this very fact makes it often a tantalizing goal.

Electron cyclotron emission, by a plasma which is far from the thermodynamic equilibrium, is an intriguing, and intrinsically complex process, determined by the electron phase-space density, and by the macroscopic magnetic field gradient along the line of sight. Given its complexity, it would be rewarding to find direct and straightforward methods for obtaining detailed microscopic information from the macroscopic radiation spectra.

The emission process is both collective and non-local. Electrons with different parallel and perpendicular momenta, and in general different energies, satisfying the resonance condition at any position along the line of sight, contribute to the emitted radiation. Moreover, the same emitting electrons can as well reabsorb the radiation emitted by their neighbours, making the resulting emission not just equal to the sum of the single contributions. It is this convolution of real space and momentum space information that causes the complexity of the emission process.

It is therefore clear that, whenever we are able to localize the spatial, and the velocity space contributions to the emitted radiation, we make a substantial progress towards the deconvolution of the microscopic information contained in the spectra. So our goal will be to look for conditions that minimize the spatial, and the momentum width of the region

determining the spectra, limiting therefore the number of the emitting electrons, and determine for this small set of electrons a unique relation between the emitted spectra and their distribution function.

2. RADIATION TEMPERATURE

The intensity of the radiation emitted by the plasma is the sum of the local contributions along the line of sight, reduced to the fraction that actually leaves the plasma,[1]

$$T_{Rad}\left(\omega, N_{||}\right) = \frac{(2\pi)^3 c^2}{\omega^2} \int_{l_1}^{l_2} dl \;\; \beta\left(l, \omega, N_{||}\right) \;\; \exp\left[-\int_{l}^{l_2} dl' \;\; \alpha\left(l', \omega, N_{||}\right)\right] , \tag{1}$$

the remaining part being reabsorbed within the plasma boundaries.
The absorption and emission coefficients, α and β,

$$\alpha \propto \sum_{s=-\infty}^{\infty} \int d^3u \;\; \frac{u_\perp}{\gamma} \;\; \delta\left(\gamma - \frac{s\,\omega_c}{\omega} - N_{||}\, u_{||}\right) \;\; \mathbf{E}^* \cdot \mathbf{T} \cdot \mathbf{E} \left(\frac{s\,\omega_c}{\omega} \frac{\partial}{\partial u_\perp} + N_{||}\, u_\perp \frac{\partial}{\partial u_{||}}\right) f ,$$

$$\beta \propto \sum_{s=-\infty}^{\infty} \int d^3u \;\; \frac{u_\perp^2}{\gamma} \;\; \delta\left(\gamma - \frac{s\,\omega_c}{\omega} - N_{||}\, u_{||}\right) \;\; \mathbf{E}^* \cdot \mathbf{T} \cdot \mathbf{E} \;\; f , \tag{2}$$

contain the microscopic information determining the emission process: it is specified by the value, and by the perpendicular and parallel derivatives of the distribution function along the resonance curve, given by the argument of the δ - function. For $N_{||} = 0$, the resonance curves are curves of constant energy (defined by the relation $\gamma = s\,\omega_c / \omega$) and, in the general case, ellipses defined by the equation

$$\frac{\left(u_{||} - \dfrac{N_{||}\left(s\omega_c / \omega\right)}{1 - N_{||}^2}\right)^2}{\dfrac{\left(s\omega_c / \omega\right)^2 - 1 + N_{||}^2}{\left(1 - N_{||}^2\right)^2}} + \frac{u_\perp^2}{\dfrac{\left(s\omega_c / \omega\right)^2 - 1 + N_{||}^2}{1 - N_{||}^2}} = 1 \;\; ; \tag{3}$$

for $N_{||} \neq 0$, the resonant energy increases monotonously moving along the resonance curve.

The polarization term appearing in the integrands,

$$\mathbf{E}^* \cdot \mathbf{T} \cdot \mathbf{E} = \left[\frac{s\, J_s(\rho)}{\rho} E_1^* + i\, J_s'(\rho) E_2^* + \frac{u_{\|}}{u_\perp} J_s(\rho) E_3^* \right] \times \left[\frac{s\, J_s(\rho)}{\rho} E_1 - i\, J_s'(\rho) E_2 + \frac{u_{\|}}{u_\perp} J_s(\rho) E_3 \right], \tag{4}$$

combined with the factor, $u_\perp^2$, acts as a weighting term of order $u_\perp^{2s}$ (the argument of the Bessel functions being $\rho = N_\perp (\omega / \omega_c) u_\perp$). The information contained in the distribution function for small perpendicular momenta has therefore less weight (the lesser, the higher the harmonic number), and for $u_\perp \approx 0$ does not influence the emission process. On the other hand when $N_{\|} \neq 0$, since the distribution function is in general a decreasing function of the energy, higher energy contributions to the integrals are exponentially smaller than lower energy ones. Combining these two properties, we obtain that for $N_{\|} \neq 0$ the integrands have a peaked structure. Its shape, for the conditions of upshifted emission discussed in the next section, turns out to be rather independent of the exact form of the distribution function, and the absorption and emission coefficients depend only on the local values of the distribution function near the (momentum space) maxima of the integrands.

The spatial width of the integrand defining the radiation temperature (1) is determined by the magnetic field gradient along the line of sight, the form of the distribution function, and the role played by reabsorption. Because of the very sensitive dependence of the resonant momenta (3) on the magnetic field value, electrons with a broad range of energies can contribute to the plasma emission, along a path parallel to the magnetic field gradient. However, for an exponential distribution function, absorption strongly depends on the number of resonant electrons, which varies exponentially with the resonant energy. Therefore, reabsorption, near a region of low resonant energy, can play a significant role in filtering the range of resonant energies, i.e., reducing the space region that contributes to the observed emission. On the other hand, viewing the plasma normally to the magnetic field gradient implies that the emitting electrons have nearly constant energies. Above some threshold resonant energy, reabsorption has almost no role in reducing the spatial width of the observable emitting region. In this case, the information contained in the emitted spectra is going to be spatially localized, only when the high energy population is spatially localized (which has to be established by other means, if possible).

In the next section we discuss conditions, for which the phase-space localization of the emitting electrons is optimal, for gaining information about the form of the distribution function.

3. UPSHIFTED ELECTRON CYCLOTRON EMISSION

3.1 Some Properties

Let's observe the electron cyclotron radiation emitted by the plasma, along a path slightly oblique with respect to magnetic field gradient ($N_{||} \neq 0$), - in a tokamak, this means using an antenna located at the low-field side of the equatorial plane, and oblique to the toroidal magnetic field, - and tune the receiver at frequencies near the fundamental, or the second harmonic cyclotron frequency.

If the parallel refractive index is not too large, and the parallel tail of the distribution not abnormally extended, only one harmonic at once will contribute to the emitted radiation, and the sum in α and β (2) will reduce to just one term. Being this the case, the emission region is determined by the resonance condition (3) corresponding to that harmonic. If x, as usual, is the coordinate along the magnetic field gradient, chosen so that $dB / dx < 0$, then the emitting electrons are located to the left of the point x_0, defined by the condition

$$\left(s\omega_c(x_0)/\omega\right)^2 - 1 + N_{||}^2 = 0 \ . \tag{5}$$

The points to the right of x_0 do not satisfy the relativistic resonance condition, and give complex resonant momenta in Eq. (3). From the condition (5), it follows that in x_0 $\omega > s\omega_c(x_c)$, and that the cyclotron resonance x_c (defined by $\omega = s\omega_c(x_c)$) is located to the left of x_0 ($x_c < x_0$), as shown in Fig. 1(a).

The layer $x \approx x_c$, for the first harmonic ordinary mode polarization, and the second harmonic extraordinary one, is strongly absorbent, and no radiation, emitted or reflected, coming from its left, can cross it. Therefore, all the observed radiation comes from the region $x_c < x < x_0$, where $\omega > s\omega_c(x_c)$, property that gives the name of "upshifted emission". The width of this region, $\Delta x = x_0 - x_c$, is determined by the value of the parallel refractive index. When $N_{||} = 0$, $x_0 = x_c$ and the emission comes from $x \approx x_c$, where the resonant energy is nearly zero: the emitting electrons belong to the bulk of the distribution function, and in this case, assuming a Maxwellian bulk, the radiation temperature is just the "electron temperature", which is usually measured by ECE temperature diagnostics. For $N_{||} \neq 0$, by increasing $\left| N_{||} \right|$, Δx and the range of the resonant energies increase as well, and the emitting electrons belong mainly to the tail of the distribution (Fig. 1(b)).

For large values of $\left| N_{||} \right|$, the spatial localization is lost because Δx is large, and moreover, since the bulk absorption coefficient decreases with increasing $\left| N_{||} \right|$, the layer $x \approx x_c$ does not act as an effective radiation dump anymore.

The range of $N_{||}$ values, allowing to obtain a space-localized emission from the electron tail, depends on the specific plasma characteristics: temperature, density,

dimensions, and the magnetic field value and gradient, i.e., on the parameters determining the fraction of radiation that is transmitted through the plasma,

$$\exp\left[-\int_{l}^{l_2} dl'\ \alpha\left(l',\omega,N_{\parallel}\right)\right]. \tag{6}$$

In order to pick up an optimal choice of observation angles, we therefore need to consider a concrete example.

3.2 Numerical Example

The case of Tore Supra, in the lower hybrid current drive regime, has been analysed extensively in Refs. 2-5. For the sake of comparison, here we consider a similar range of parameters:

$$R = 225\,\text{cm}, \quad a = 70\ \text{cm},$$
$$n_e(r) = 2\times10^{13}\left(1-r^2/a^2\right)\ \text{cm}^{-3}, \quad T_e(r) = 3\ \left(1-r^2/a^2\right)^{3/2}\ \text{keV},$$
$$B(0) = 3.93\,\text{T}, \quad Z_{eff} = 1\ .$$

In order to simulate the non-thermal radiation spectra during the current drive regime, we compute the electron distribution function with a 3D Fokker-Planck code, assuming the following model for the lower hybrid spectrum,

$$D_{LH} = 0.8 \quad \text{for} \quad u_1 < u_{\parallel} < u_2, \quad \text{with}$$
$$u_1 = 3.5\left(T_e(0)/T_e(r)\right)^{1/2}, \ \text{and} \quad u_2 = 7\left(T_e(0)/T_e(r)\right)^{1/2}.$$

The numerical distribution function is then inserted in the absorption and emission coefficients (2), and the emitted spectra are computed from the equation of radiation transport (1).

If the receiving antenna is rotated at an angle $\psi \approx 70^\circ - 75^\circ$, with respect to the toroidal magnetic field, good phase-space localization of the non-thermal radiation spectra is achieved. This is demonstrated in Figs. 2(a) and 2(b), where the parallel momentum localization of α and β, and the spatial localization of the emitting electrons is shown, for second harmonic, extraordinary mode radiation. The corresponding emission spectra (f_{FP}) are plotted in Fig. 3(a): the radiation temperature appears to be well above that of a Maxwellian having the bulk temperature (f_M), for frequencies corresponding to emission from the central part of the plasma. Smaller emission angles will give even better spatial localization, but will decrease the non-thermal component of the radiation; on the contrary,

larger angles will increase the non-thermal contribution, but the spatial localization will worsen. Our choice represents the best compromise between these two conflicting requirements, for the given conditions.

In the next section we will try to establish how much, and what information about the distribution function, is possible to extract from these spectra.

4. INVERSION OF THE ELECTRON DISTRIBUTION

4.1 Principles

When the integrand defining the radiation temperature (1) is sharply peaked, as in the case discussed in the previous section, it is possible to relate the radiation temperature, which is a global quantity, to the local values of the absorption and emission coefficients:

$$\begin{aligned} T_{Rad}(\omega,N_{\parallel}) &= \int_{l_1}^{l_2} dl\ T_{Rad}^{loc}(l,\omega,N_{\parallel})\ \alpha(l,\omega,N_{\parallel}) \exp\left[-\int_{l}^{l_2} dl'\ \alpha(l',\omega,N_{\parallel})\right] \\ &\approx T_{Rad}^{loc}(\bar{l},\omega,N_{\parallel})\ \int_{l_1}^{l_2} dl\ \alpha(l,\omega,N_{\parallel}) \exp\left[-\int_{l}^{l_2} dl'\ \alpha(l',\omega,N_{\parallel})\right] \\ &= T_{Rad}^{loc}(\bar{l},\omega,N_{\parallel})\left(1-\exp\left[-\int_{l_1}^{l_2} dl'\ \alpha(l',\omega,N_{\parallel})\right]\right), \end{aligned} \tag{7}$$

through the local radiation temperature,

$$T_{Rad}^{loc}(\bar{l},\omega,N_{\parallel}) = \frac{(2\pi)^3 c^2}{\omega^2}\beta(\bar{l},\omega,N_{\parallel}) / \alpha(\bar{l},\omega,N_{\parallel}), \tag{8}$$

calculated at the point $\bar{l}$, where the integrand is maximum. For a Maxwellian distribution function this quantity is just the electron temperature at the point $\bar{l}$. In the general case, we can split the distribution function into the sum of its Maxwellian and non-Maxwellian parts, $f = f_M + f_{NM}$, and, splitting in the same way α and β, we obtain the general relation

$$\begin{aligned} \frac{1}{T_{Rad}^{loc}} &= \frac{(2\pi)^3 c^2}{\omega^2}\frac{\alpha}{\beta} = \frac{(2\pi)^3 c^2}{\omega^2}\left\{\left(1-\frac{\beta_{NM}}{\beta}\right)\frac{\alpha_M}{\beta_M} + \frac{\beta_{NM}}{\beta}\frac{\alpha_{NM}}{\beta_{NM}}\right\} \\ &= \left(1-\frac{1}{1+\beta_M/\beta_{NM}}\right)\frac{1}{T_e} + \frac{1}{1+\beta_M/\beta_{NM}}\frac{1}{T_{NM}}, \end{aligned} \tag{9}$$

which shows that the the inverse of the local radiative temperature varies linearly between the inverse of the bulk temperature and of the non-Maxwellian temperature, depending on the relative strength of the two emission coefficients. One has to note that the non-Maxwellian temperature,

$$T_{NM} = \frac{(2\pi)^3 c^2}{\omega^2} \beta_{NM} / \alpha_{NM} \ , \tag{10}$$

is a function of the momentum, through the resonant momenta at the point $\bar{l}$, and not a constant, as in the Maxwellian case.

We can take advantage of the good momentum localization of the upshifted emission, by looking for an expansion of the distribution function, near the maxima of the α and β integrands, say a Taylor expansion around the point $\left(u_{\|} = u_{\|0}, u_{\perp}^2 = 0\right)$:

$$\begin{aligned} &\ln\left(f - C_N f_M\right) \\ &\approx c + c_{\|}\left(u_{\|} - u_{\|0}\right) + c_{\perp} u_{\perp}^2 + c_{\|\|}\left(u_{\|} - u_{\|0}\right)^2 + c_{\|\perp}\left(u_{\|} - u_{\|0}\right) u_{\perp}^2 + c_{\perp\perp} u_{\perp}^4 + \ldots , \end{aligned} \tag{11}$$

where C_N is a normalization constant. Inserting this expansion in the expression for the local radiation temperature, we get a Kirchhoff-like law for the non-Maxwellian radiation temperature,

$$\begin{aligned} \frac{1}{T_{NM}} = \frac{2}{m_e c^2} \Big\{ &\left(s\,\omega_c / \omega\right)\left[c_{\perp} + c_{\|\perp}\left\langle u_{\|} - u_{\|0}\right\rangle + 2\, c_{\perp\perp}\left\langle u_{\perp}^2\right\rangle + \ldots\right] \\ &+ N_{\|}\left[\tfrac{1}{2}\, c_{\|} + c_{\|\|}\left\langle u_{\|} - u_{\|0}\right\rangle + \tfrac{1}{2}\, c_{\perp\perp}\left\langle u_{\perp}^2\right\rangle + \ldots\right]\Big\} \ . \end{aligned} \tag{12}$$

The averaging, $\langle \ldots \rangle$, is performed with the integral operator (2) defining β. In this way, the equation for the local radiative temperature, (7), (9), would have been reduced to an algebrical equation, if we could ignore the dependence of β_{NM} on the the expansion coefficients; this is clearly not the case. Moreover, the exact position of the point of maximum, $\bar{l}$, where we are going to solve the problem, is determined by β_{NM}. To reduce this complicated dependence, we proceed as it follows.

If we initially assume an approximate distribution function, and compute with it β_{NM} (and α_{NM}), we can get the position of the maximum, $\bar{l}$; then solve our equation for the expansion coefficients, obtain a new approximation for the distribution, and iterate the procedure. In order to have a well posed problem, we need a number of experimental emission spectra, at least equal to the number of coefficients we want to use in the expansion.

The information contained in the various spectra has to be independent, i.e., the respective β (or α) maxima don't have to overlap.

That this procedure can be convergent is shown in the next section. Here, we would only like to comment that an approximation for β_{NM} is less tricky than one for T_{NM}, since the former depends only on the value of the distribution function, while the latter depends on the derivatives as well.

4.2 Numerical Result

In this section, we present the numerical solution of inverse problem for the electon cyclotron emission, for the conditions discussed earlier in Sec. 3-2. As input data, we consider the set of four upshifted emissions plotted in Figs. 3(a) and 3(b), corresponding to the first harmonic ordinary mode polarization, and the second harmonic extraordinary one, and two observation angles, $\psi = 70^\circ$ and 75°, with respect to the toroidal magnetic field. Equations (7), (9), and (12) allow us to write a set of four equations for the input emissions.

A minimization iterative code was written to solve the system of equations. The solution was calculated for different numbers of coefficients in the local expansion of the distribution function (11). It appeared possible to obtain a very good solution with just three coefficients. The emission spectra, computed from this solution, are shown in Figs. 3(a) and 3(b) (f_{inv}), and compare very well with the input spectra, obtained from the Fokker-Planck computed distribution function (f_{FP}). However, what is even more startling is the comparison between the two distribution functions, near the phase-space maximum of the emission.

In Fig. 4, the level curves of the inverted distribution function are plotted near the resonant region, for $x = 0$. Also shown are the sections of the resonance curves, that contain 99% of the contribution to the emission; the emission maxima are indicated with a marker ($\circ$). The inverted distribution function is compared in Fig. 5, with the Fokker-Planck distribution along these sections. The agreement is excellent in the lower energy part, near to the emission maxima, and not bad at higher energies. The good space localization of the emission region, shown in Fig. 2(b), makes it possible to obtain from the inversion procedure the radial dependence of the distribution function. This is demonstrated in Fig. 6, where the Fokker-Planck and the inverted distribution functions are plotted along the sections of the resonance curves at two different radial positions.

In conclusion, the result clearly shows that the inversion process is effective in determining the local structure of the distribution function, in the momentum space region responsible for the emission process. Outside that region, we have no reason to expect agreement, since the inversion process is independent of the information contained there. However, if the distribution function is smooth enough, as in this particular case, the local

expansion of the distribution (11) is not a bad approximation even at larger energies, as shown in Fig. 7, where the level curves of the two distributions are plotted for $x = 0$.

5. CONCLUSIONS

The numerical study presented in this paper, by showing the possibility to invert the electron distribution function from a small set of upshifted non-thermal emission spectra - computed through a Fokker-Planck code for a lower hybrid current drive regime - indicates the potential of the method: no ad-hoc models, or assumptions are necessary in order to get a precise description of the distribution function, in the phase-space region responsible for the electron cyclotron emission.

The major point that remains to be clarified is the robustness of the algorithm, vis-à-vis real non-thermal emission spectra, which are noisy, and, because of finite antenna resolution, contain space averaged information. Another point, that needs to be addressed, is the class of distribution functions, describing different regimes, and different generating mechanisms of the suprathermal electrons, to which the method is applicable.

It is obvious that experimental results will be the major factor in understanding the problem. So far, the only experimental setup,[6,7] that comes close to the requirements presented in this paper, does not have the flexibility to investigate the upshifted emission for variable angles, and the chosen observation angles, $\Delta\psi = \pm 15^\circ$ with respect to the normal, are too small to be really effective.

References

1 G. Bekefi, *Radiation Processes in Plasmas* (Wiley, New York, 1966).

2 I. Fidone, G. Giruzzi, V. Krivenski, E. Mazzucato, and L.F. Ziebell, Nucl. Fusion **27**, 579 (1987).

3 G. Giruzzi, I. Fidone, and R.L. Meyer, Nucl. Fusion **29**, 1381 (1989).

4 I. Fidone, and G. Giruzzi, Nucl. Fusion **30**, 803 (1990).

5 G. Giruzzi, I. Fidone, and M.J. Marchã, Nucl. Fusion **31**, 517 (1991).

6 L. Rodriguez, N. Augé, G. Giruzzi, C. Javon, L. Laurent, and M. Talvard, in *Controlled Fusion and Plasma Physics* (Proc. 18th Europ. Conf., Berlin, 1991), Vol. 15C, Part IV, 353.

7 M. Talvard, G. Giruzzi, and W.D. Liu, in *Controlled Fusion and Plasma Physics*, (Proc. 19th Europ. Conf., Innsbruck 1992), Vol. 16C, Part II, 1103.

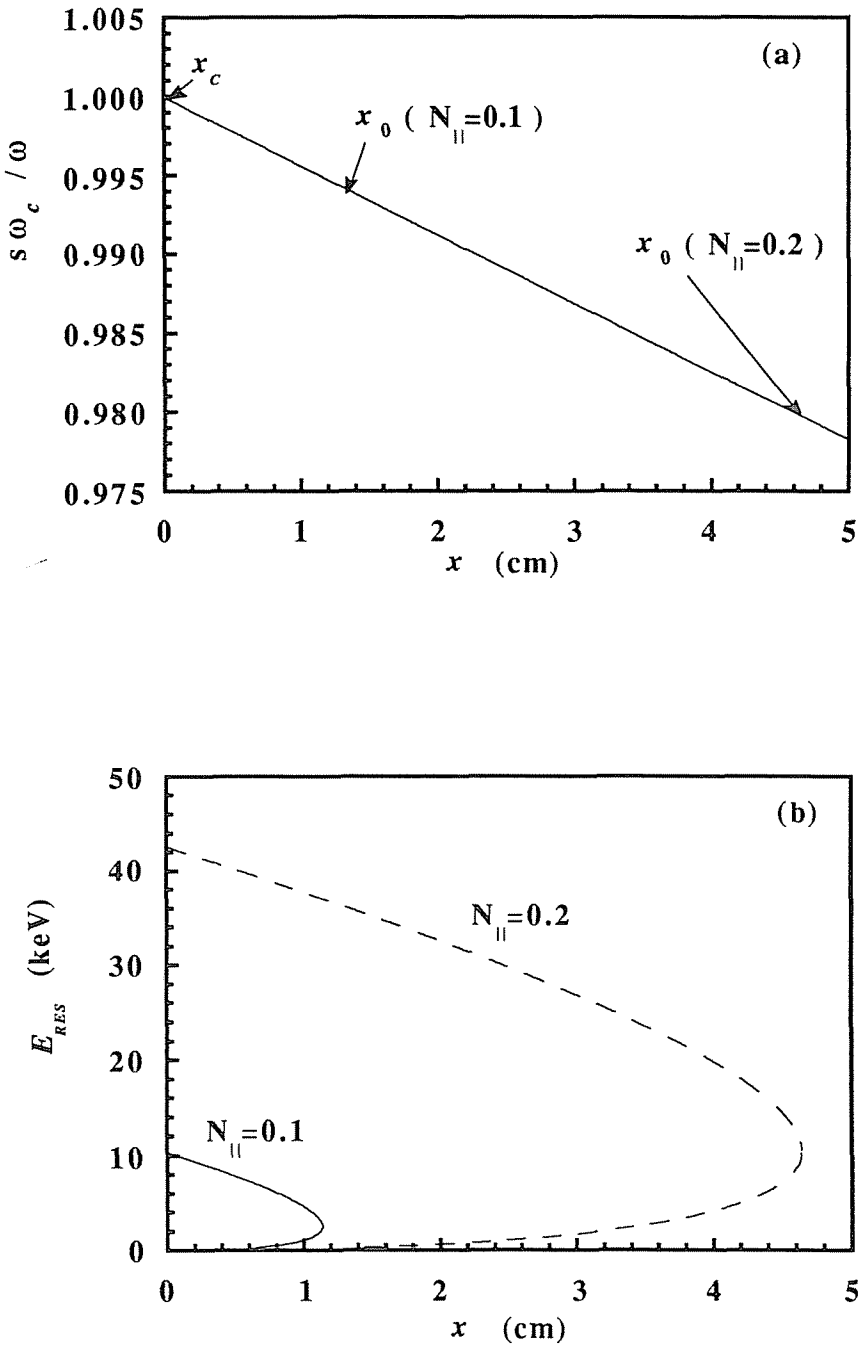

Fig.1(a) Upshifted emission region, $x_c < x < x_0$, in a tokamak-like plasma, for $N_{||} = 0.1$, and 0.2. (b) Minimum and maximum resonant energy vs position, for the same parameters.

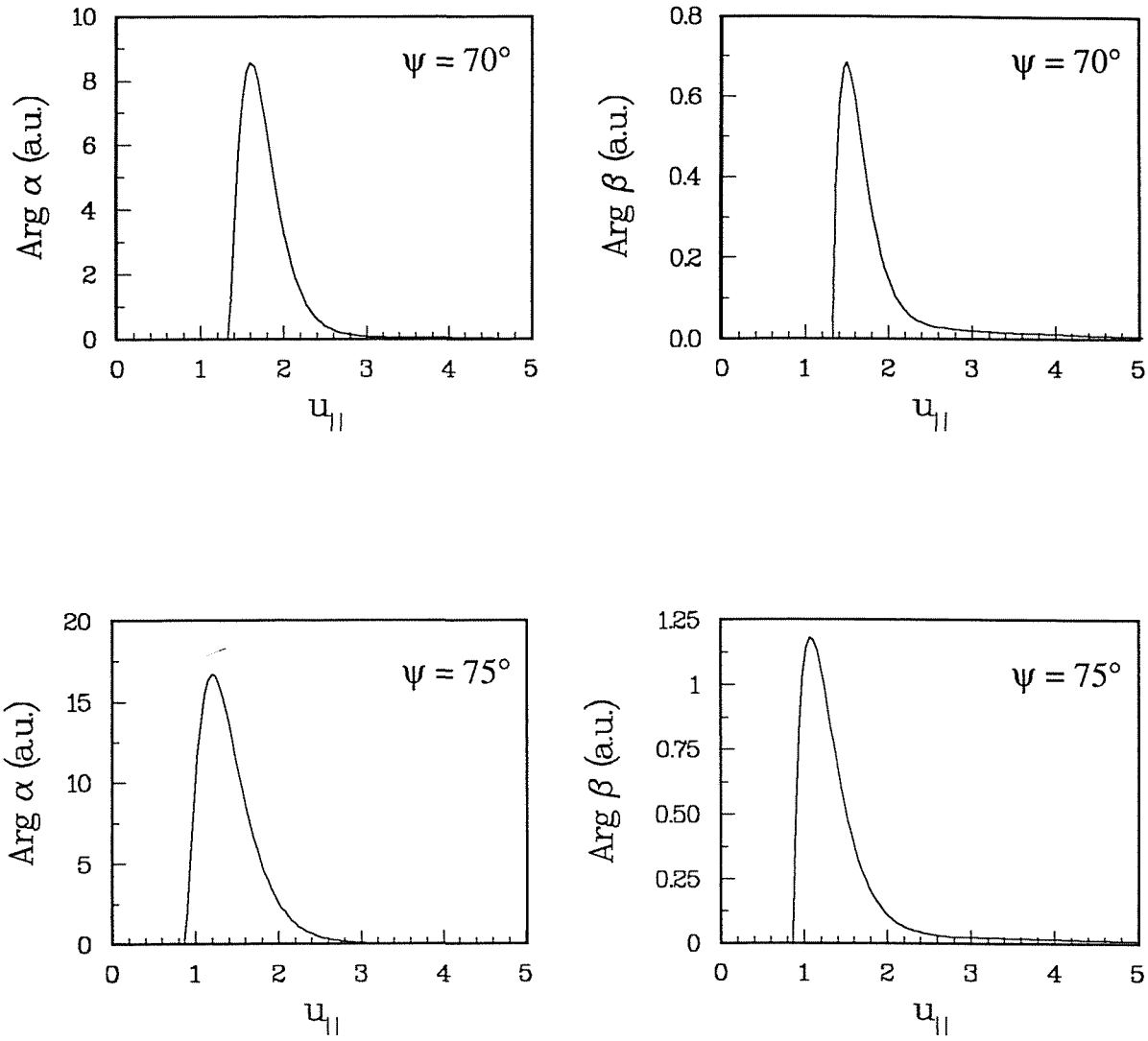

Fig.2(a) α and β integrands along the resonance curve, parameterized by the parallel momentum $u_{\|} = p_{\|} / \sqrt{m_e T_e}$, for the second harmonic extraordinary mode, at r=0.

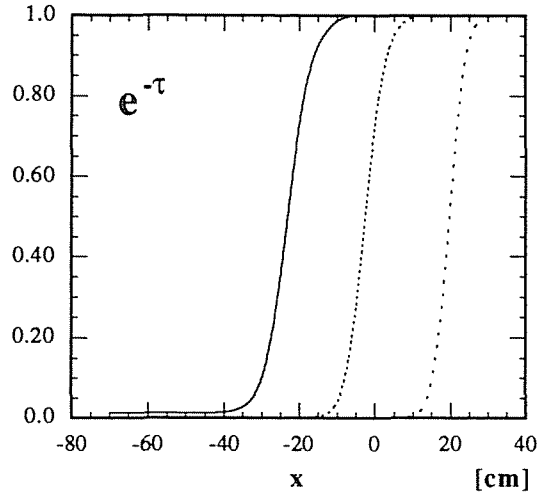

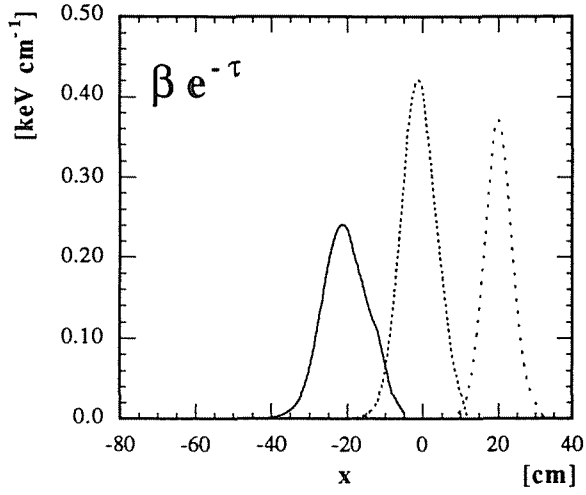

$\psi = 70°$, solid line υ = 252.73 GHz, dashed line υ = 230.32 GHz, dotted line υ = 207.60 GHz

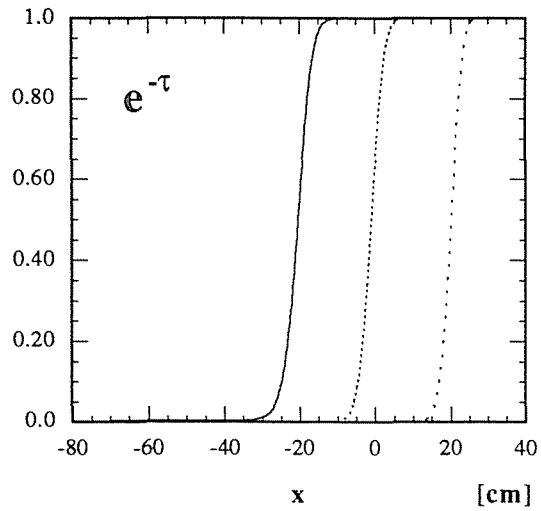

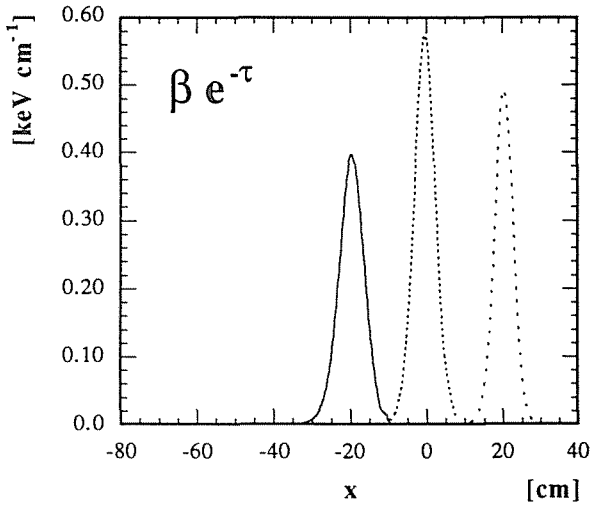

$\psi = 75°$, solid line υ = 246.61 GHz, dashed line υ = 225.48 GHz, dotted line υ = 205.08 GHz

Fig.2(b) Integrands defining the radiation temperature, and attenuation factors vs position, for the second harmonic extraordinary mode.

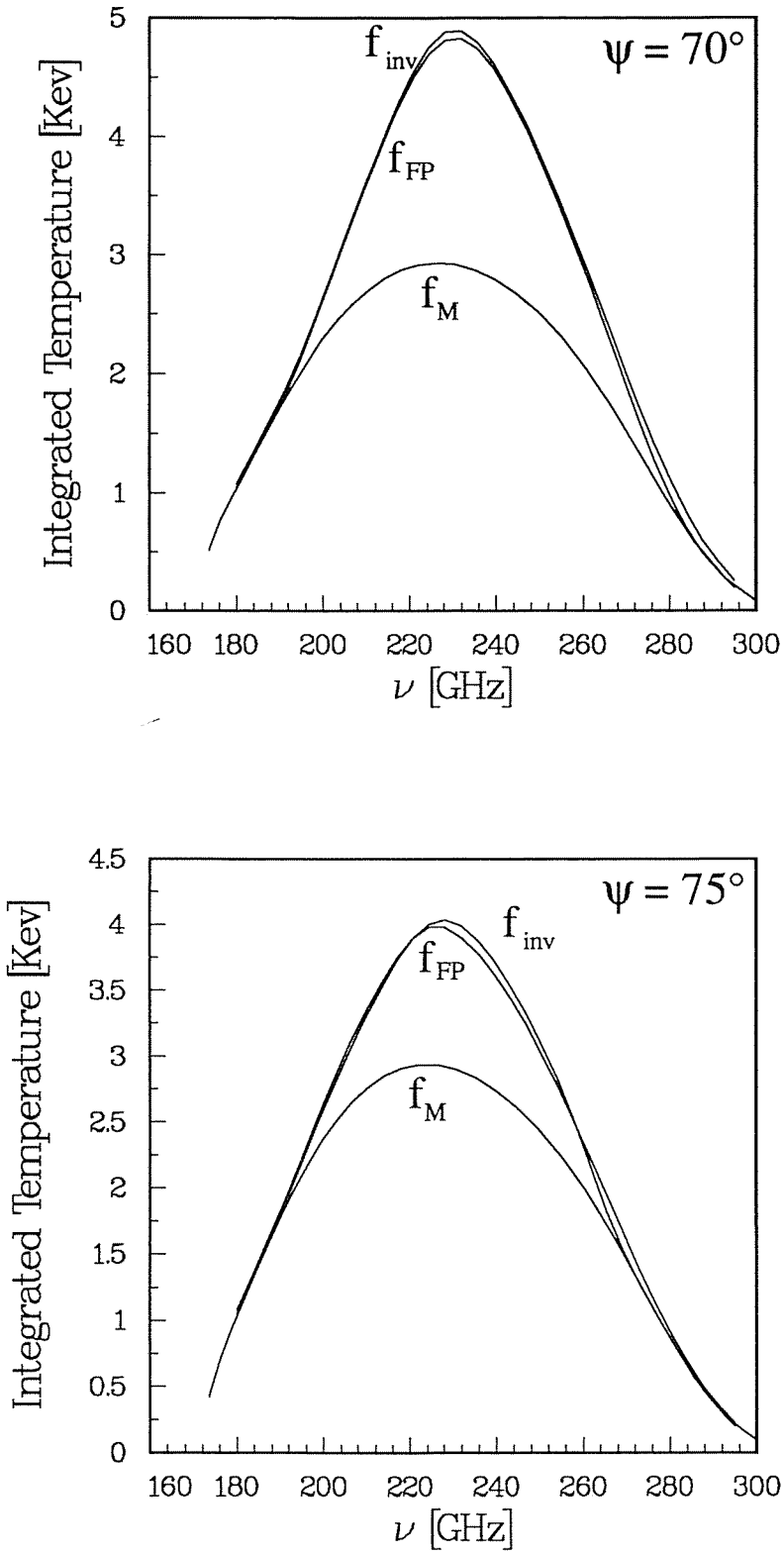

Fig.3(a) Emission spectra for the second harmonic extraordinary mode, and various distribution functions: (f_M) for a Maxwellian plasma, (f_{FP}) for the Fokker-Planck distribution function, (f_{inv}) for the solution of the inversion problem.

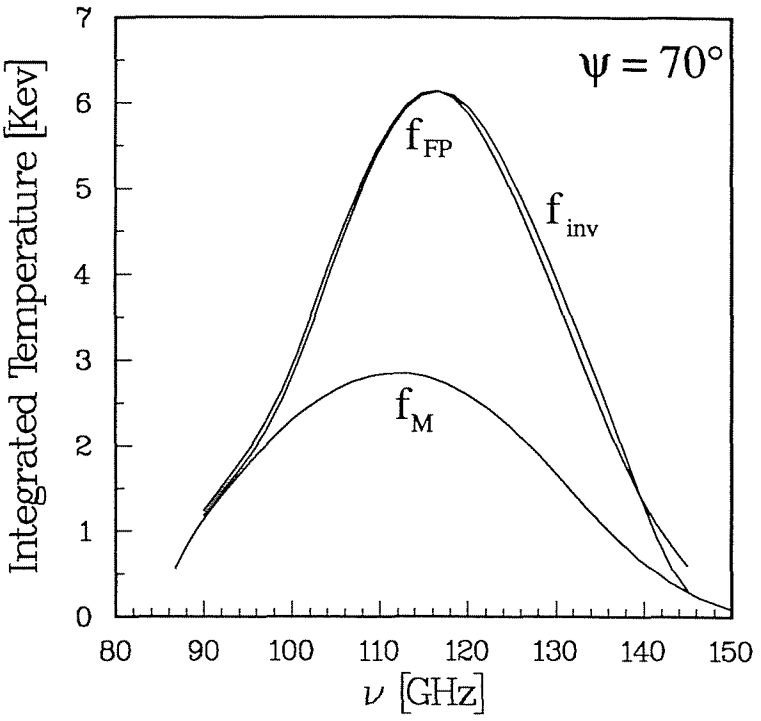

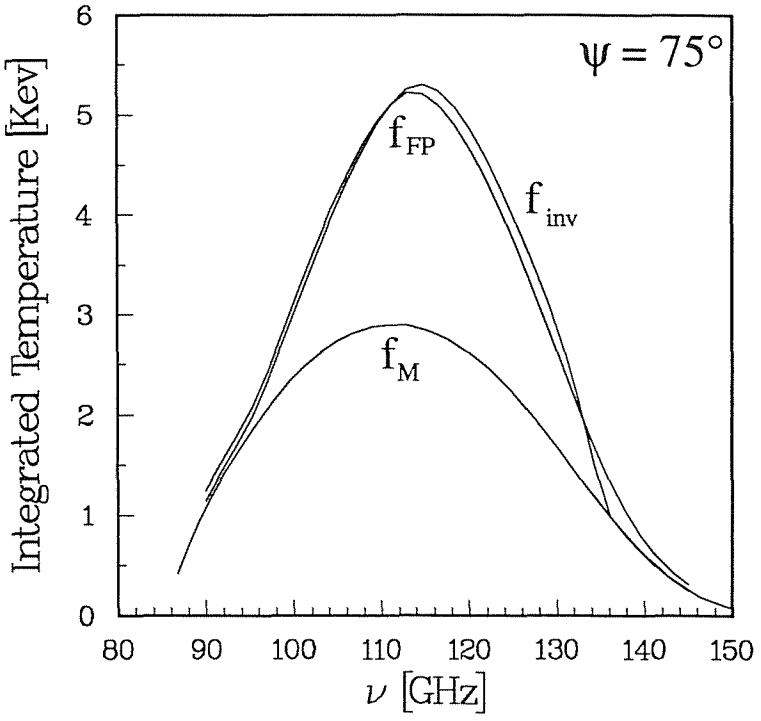

Fig.3(b) Emission spectra for the first harmonic ordinary mode, and various distribution functions: (f_M) for a Maxwellian plasma, (f_{FP}) for the Fokker-Planck distribution function, (f_{inv}) for the solution of the inversion problem.

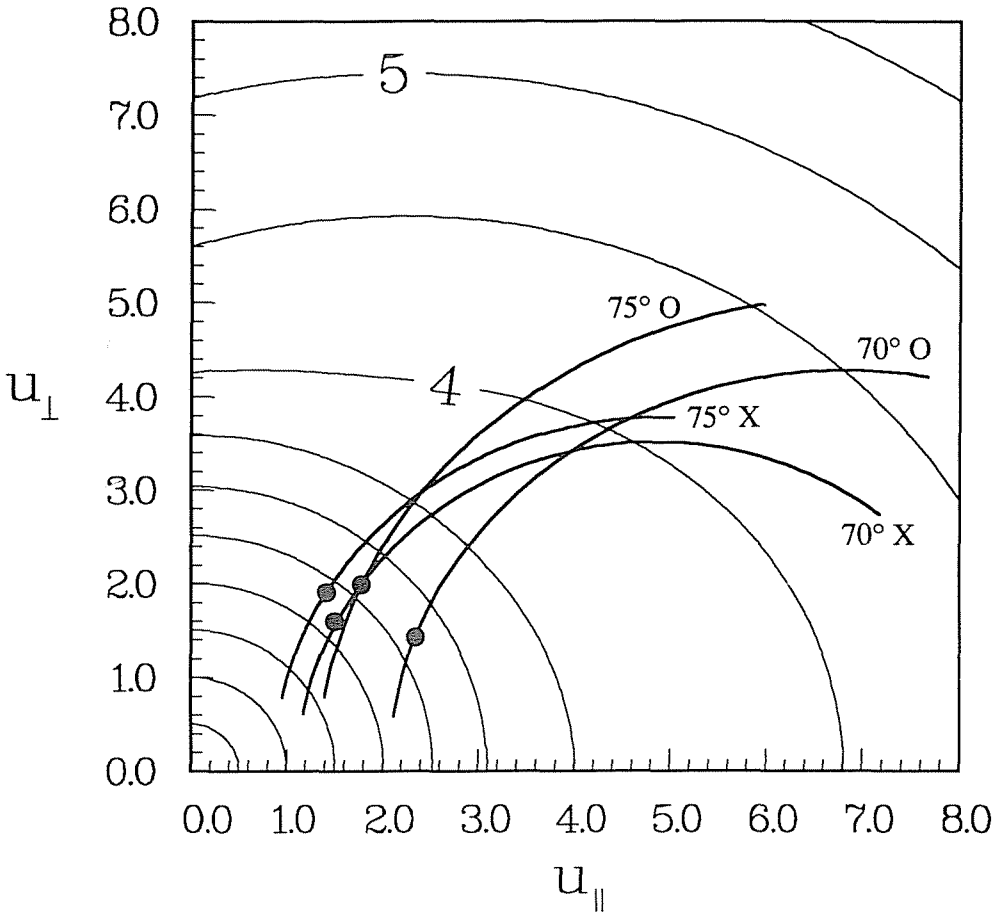

Fig.4 Level curves of the inverted distribution function near the resonant region, and sections of the resonance curves, containing 99% of the contribution to the emitted spectra, at r = 0 (for each resonance curve, the frequency is chosen so that the corresponding emission has its maximum contribution at r = 0). The position of the emission maxima (•) are also shown.

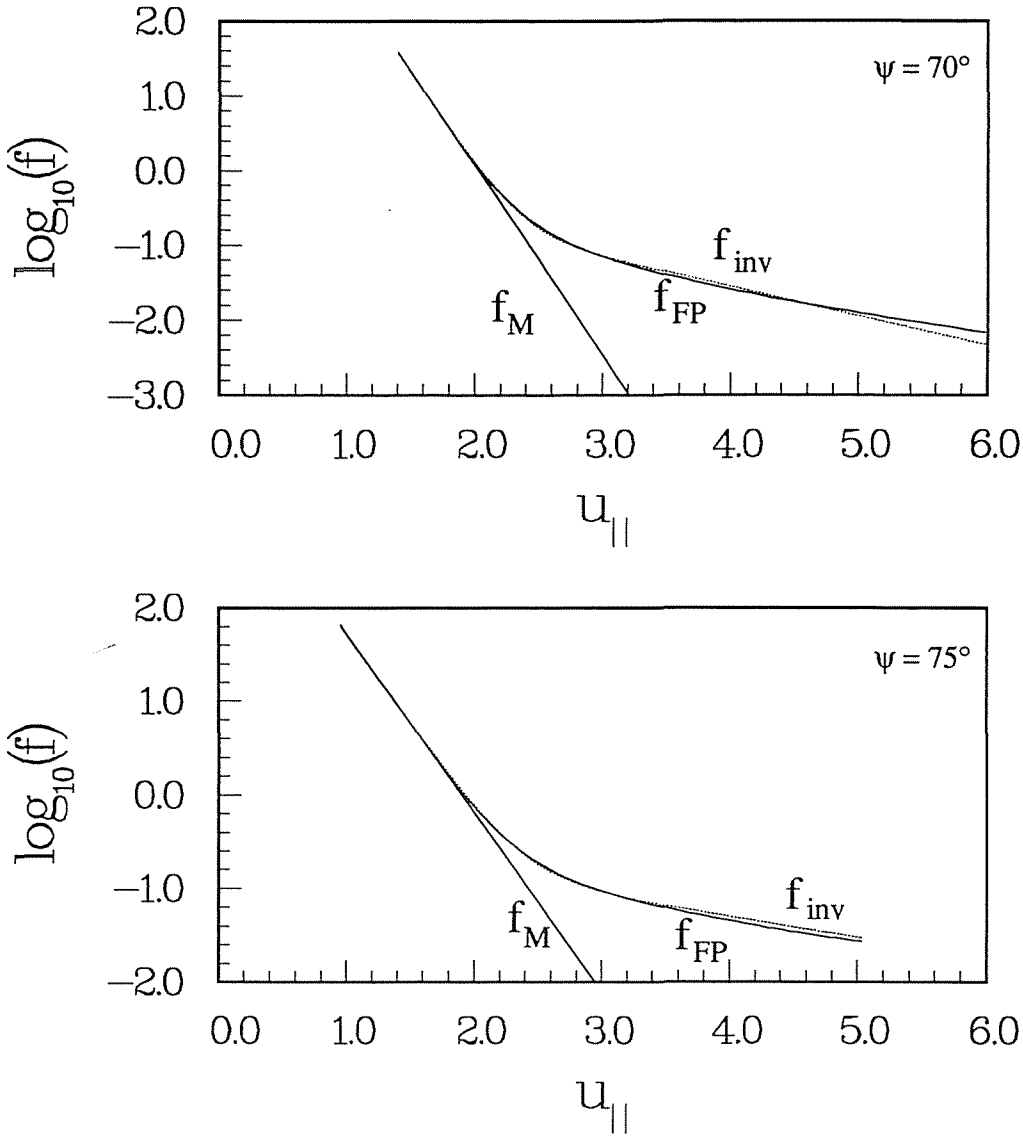

Fig.5(a) Comparison between the Fokker-Planck and the inverted distribution functions, along the resonance curves plotted in Fig.4, for second harmonic extraordinary mode.

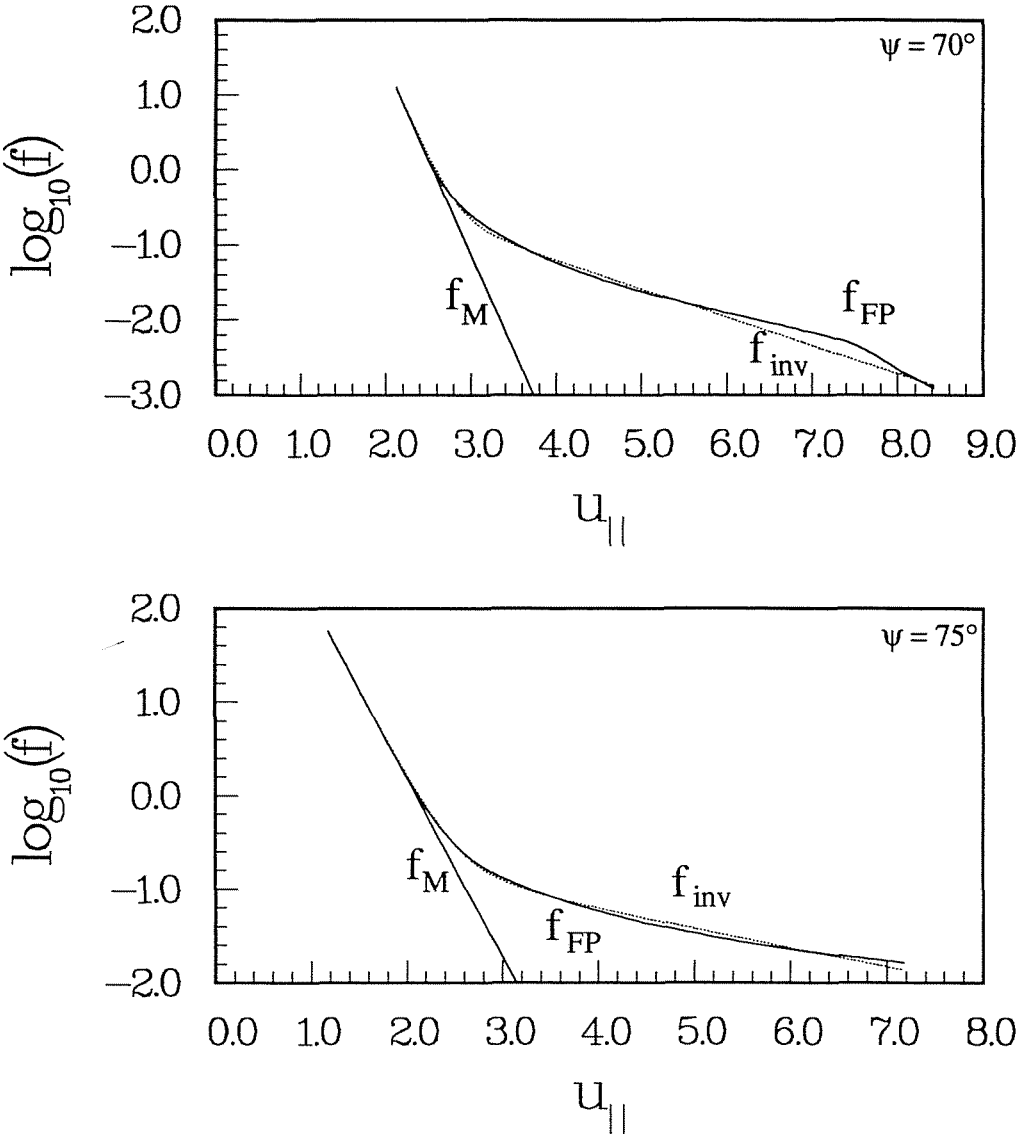

Fig.5(b) Comparison between the Fokker-Planck and the inverted distribution functions, along the resonance curves plotted in Fig.4, for the first harmonic ordinary mode.

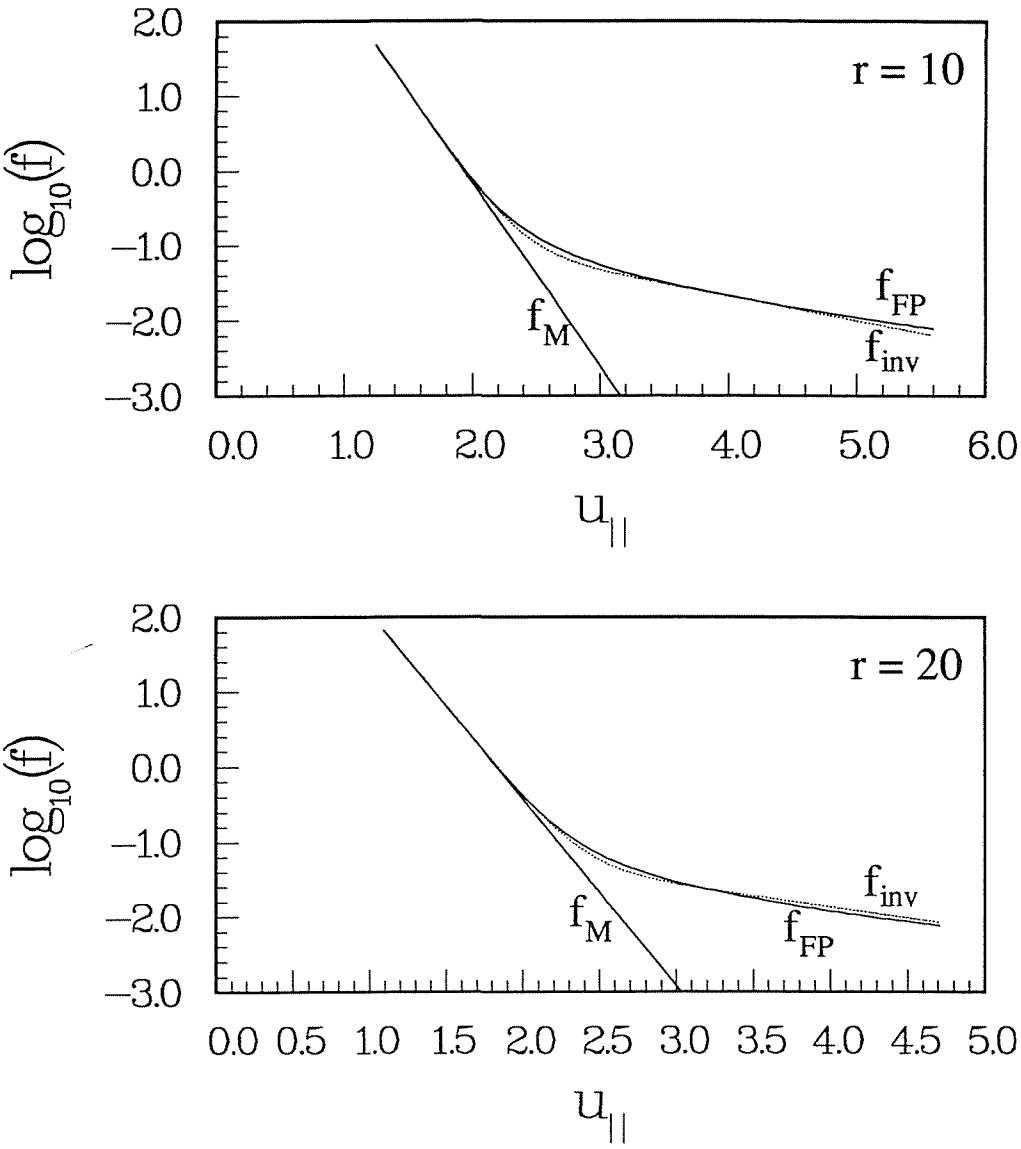

Fig.6 Comparison between the Fokker-Planck and the inverted distribution function, along the resonance curves, for the extraordinary mode, $\psi = 70°$, at two different radial positions.

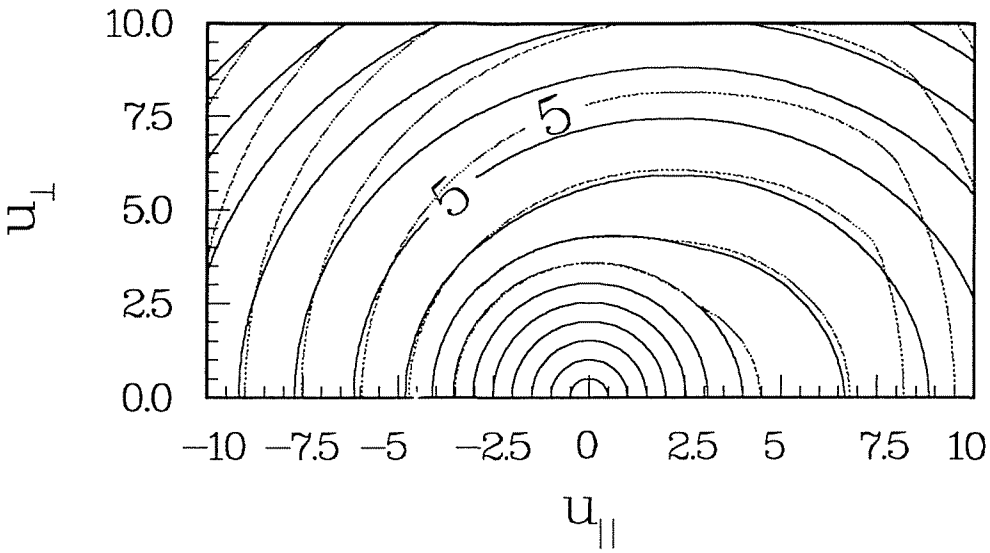

Fig.7 Level curves of the inverted distribution function (solid curves) and of the Fokker-Planck distribution (dashed curves), at r = 0.

CIEMAT-713

Centro de Investigaciones Energéticas, Medioambientales y Tecnológicas
Instituto de Investigación Básica. Madrid

"Radial profile of the electron distribution from electron cyclotron emission measurements".

TRIBALDOS, V.; KRIVENSKI, V. (1993) 19 pp.; 7 figs.; 7 refs.
A numerical study is presented, showing the possibility to invert the electron distribution function from a small set of non-thermal spectra, for a regime of lower hybrid current drive.

DOE CLASSIFICATION AND DESCRIPTORS: 700350. Cyclotron Radiation. Electron Cyclotron-resonance. Distribution Functions. Hybrid systems. Current-drive heating. Numerical Analysis.

CIEMAT-713

Centro de Investigaciones Energéticas, Medioambientales y Tecnológicas
Instituto de Investigación Básica. Madrid

"Radial profile of the electron distribution from electron cyclotron emission measurements".

TRIBALDOS, V.; KRIVENSKI, V. (1993) 19 pp.; 7 figs.; 7 refs.
A numerical study is presented, showing the possibility to invert the electron distribution function from a small set of non-thermal spectra, for a regime of lower hybrid current drive.

DOE CLASSIFICATION AND DESCRIPTORS: 700350. Cyclotron Radiation. Electron Cyclotron-resonance. Distribution Functions. Hybrid systems. Current-drive heating. Numerical Analysis.

CIEMAT-713

Centro de Investigaciones Energéticas, Medioambientales y Tecnológicas
Instituto de Investigación Básica. Madrid

"Radial profile of the electron distribution from electron cyclotron emission measurements".

TRIBALDOS, V.; KRIVENSKI, V. (1993) 19 pp.; 7 figs.; 7 refs.
A numerical study is presented, showing the possibility to invert the electron distribution function from a small set of non-thermal spectra, for a regime of lower hybrid current drive.

DOE CLASSIFICATION AND DESCRIPTORS: 700350. Cyclotron Radiation. Electron Cyclotron-resonance. Distribution Functions. Hybrid systems. Current-drive heating. Numerical Analysis.

CIEMAT-713

Centro de Investigaciones Energéticas, Medioambientales y Tecnológicas.
Instituto de Investigación Básica. Madrid.

"Perfil radial de la función de distribución electrónica mediante medidas de emisión a la frecuencia ciclotrónica electrónica".

TRIBALDOS, V.; KRIVENSKI, V. (1993) 19 pp.; 7 figs.; 7 refs.
Se presenta un estudio mostrando la posibilidad de invertir la función de distribución electrónica a partir de un pequeño conjunto de emisiones no térmicas para un régimen de inducción de corriente mediante lower hybrid.

CLASIFICACION DOE Y DESCRIPTORES: 700350. Cyclotron Radiation. Electron Cyclotron-resonance. Distribution Functions. Hybrid Systems. Current-drive Heating. Numerical Analysis.

CIEMAT-713

Centro de Investigaciones Energéticas, Medioambientales y Tecnológicas.
Instituto de Investigación Básica. Madrid.

"Perfil radial de la función de distribución electrónica mediante medidas de emisión a la frecuencia ciclotrónica electrónica".

TRIBALDOS, V.; KRIVENSKI, V. (1993) 19 pp.; 7 figs.; 7 refs.
Se presenta un estudio mostrando la posibilidad de invertir la función de distribución electrónica a partir de un pequeño conjunto de emisiones no térmicas para un régimen de inducción de corriente mediante lower hybrid.

CLASIFICACION DOE Y DESCRIPTORES: 700350. Cyclotron Radiation. Electron Cyclotron-resonance. Distribution Functions. Hybrid Systems. Current-drive Heating. Numerical Analysis.

CIEMAT-713

Centro de Investigaciones Energéticas, Medioambientales y Tecnológicas.
Instituto de Investigación Básica. Madrid.

"Perfil radial de la función de distribución electrónica mediante medidas de emisión a la frecuencia ciclotrónica electrónica".

TRIBALDOS, V.; KRIVENSKI, V. (1993) 19 pp.; 7 figs.; 7 refs.
Se presenta un estudio mostrando la posibilidad de invertir la función de distribución electrónica a partir de un pequeño conjunto de emisiones no térmicas para un régimen de inducción de corriente mediante lower hybrid.

CLASIFICACION DOE Y DESCRIPTORES: 700350. Cyclotron Radiation. Electron Cyclotron-resonance. Distribution Functions. Hybrid Systems. Current-drive Heating. Numerical Analysis.

CIEMAT-713

Centro de Investigaciones Energéticas, Medioambientales y Tecnológicas.
Instituto de Investigación Básica. Madrid.

"Perfil radial de la función de distribución electrónica mediante medidas de emisión a la frecuencia ciclotrónica electrónica".

TRIBALDOS, V.; KRIVENSKI, V. (1993) 19 pp.; 7 figs.; 7 refs.
Se presenta un estudio mostrando la posibilidad de invertir la función de distribución electrónica a partir de un pequeño conjunto de emisiones no térmicas para un régimen de inducción de corriente mediante lower hybrid.

CLASIFICACION DOE Y DESCRIPTORES: 700350. Cyclotron Radiation. Electron Cyclotron-resonance. Distribution Functions. Hybrid Systems. Current-drive Heating. Numerical Analysis.